



# Cardiac mTOR complex 2 preserves ventricular function in pressure-overload hypertrophy

Pankaj Shende<sup>1†</sup>, Lifen Xu<sup>1†</sup>, Christian Morandi<sup>1†</sup>, Laura Pentassuglia<sup>1</sup>, Philippe Heim<sup>1</sup>, Sonia Lebboukh<sup>1</sup>, Corinne Berthonneche<sup>2</sup>, Thierry Pedrazzini<sup>2</sup>, Beat A. Kaufmann<sup>1</sup>, Michael N. Hall<sup>3</sup>, Markus A. Ruegg<sup>3</sup>, and Marijke Brink<sup>1\*</sup>

<sup>1</sup>Department of Biomedicine, University of Basel and University Hospital Basel, Hebelstrasse 20, CH-4031 Basel, Switzerland; <sup>2</sup>Department of Medicine and Cardiovascular Assessment Facility, University of Lausanne Medical School, Lausanne, Switzerland; and <sup>3</sup>Biozentrum, University of Basel, Basel, Switzerland

Received 8 January 2015; revised 16 October 2015; accepted 6 November 2015; online publish-ahead-of-print 23 November 2015

Time for primary review: 43 days

## Aims

Mammalian target of rapamycin (mTOR), a central regulator of growth and metabolism, has tissue-specific functions depending on whether it is part of mTOR complex 1 (mTORC1) or mTORC2. We have previously shown that mTORC1 is required for adaptive cardiac hypertrophy and maintenance of function under basal and pressure-overload conditions. In the present study, we aimed to identify functions of mTORC2 in the heart.

## Methods and results

Using tamoxifen-inducible cardiomyocyte-specific gene deletion, we generated mice deficient for cardiac rapamycin-insensitive companion of mTOR (riCTOR), an essential and specific component of mTORC2. Under basal conditions, rictor deficiency did not affect cardiac growth and function in young mice and also had no effects in adult mice. However, transverse aortic constriction caused dysfunction in the rictor-deficient hearts, whereas function was maintained in controls after 1 week of pressure overload. Adaptive increases in cardiac weight and cardiomyocyte cross-sectional area, fibrosis, and hypertrophic and metabolic gene expression were not different between the rictor-deficient and control mice. In control mice, maintained function was associated with increased protein levels of rictor, protein kinase C (PKC) $\beta$ II, and PKC $\delta$ , whereas *rictor* ablation abolished these increases. *Rictor* deletion also significantly decreased PKC $\epsilon$  at baseline and after pressure overload. Our data suggest that reduced PKC $\epsilon$  and the inability to increase PKC $\beta$ II and PKC $\delta$  abundance are, in accordance with their known function, responsible for decreased contractile performance of the rictor-deficient hearts.

## Conclusion

Our study demonstrates that mTORC2 is implicated in maintaining contractile function of the pressure-overloaded male mouse heart.

## Keywords

Heart failure • Hypertrophy • Metabolism • Signal transduction

## 1. Introduction

Recent studies have identified mammalian target of rapamycin (mTOR) as an important regulator of cardiac adaptations to pressure overload.<sup>1</sup> mTOR, an evolutionary conserved serine/threonine kinase belonging to the phosphatidylinositol 3-kinase (PI3K)-related kinase family of proteins, matches cell growth and metabolism with environmental resources and other cues.<sup>2</sup> Thus, it senses nutrient and energy status, growth factors, oxygen levels and stress, and adapts a range of cellular functions related to growth and metabolism correspondingly. In line with its important regulatory function, mTOR overexpression is

protective in pressure-overloaded mouse hearts,<sup>3</sup> whereas conditional mTOR deletion causes cardiac dysfunction.<sup>4</sup>

mTOR has different functions depending on whether it is part of the multiprotein complex termed mTOR complex 1 (mTORC1) or mTORC2.<sup>5,6</sup> We recently showed that raptor (regulatory-associated protein of mTOR) is required for basal cardiac function and that adequate mTORC1 activity is even more critical in the pressure-overloaded heart. Reduced mTORC1 activity in raptor-deficient cardiomyocytes leads to heart failure and death within 2 weeks of aortic constriction.<sup>7</sup> While increased autophagy and apoptosis as well as changed metabolism were observed in the raptor-deficient hearts, one of the primary reasons

\* Corresponding author. Tel: +41 61 265 33 61; fax: +41 61 265 23 50, E-mail: marijke.brink@unibas.ch

† The first three authors equally contributed to this work.

Published on behalf of the European Society of Cardiology. All rights reserved. © The Author 2015. For permissions please email: journals.permissions@oup.com.

for the observed dysfunction is reduced protein synthesis and a lack of adaptive hypertrophy.<sup>7</sup>

Much less is known about mTORC2 owing to the unavailability of selective inhibitors. Early work demonstrated that by phosphorylating members of the AGC kinase family such as protein kinase C (PKC), PKB/Akt, and SGK1, mTORC2 regulates cytoskeletal actin organization, cell survival, and other processes.<sup>8</sup> The availability of tissue-specific knockout models for essential components of mTORC2 has recently given more insights into the *in vivo* functions of mTORC2 for some tissues. Knockout of the mTORC2 component rapamycin-insensitive companion of mTOR (riCTOR) in skeletal muscle showed either no phenotype<sup>9</sup> or impaired insulin-stimulated glucose transport and enhanced glycogen synthase activity.<sup>10</sup> Adipose-specific rictor-deficient mice showed increased body size, an enlarged pancreas, and hyperinsulinaemia,<sup>10,11</sup> whereas liver-specific rictor knockout mice revealed that mTORC2 regulates hepatic glucose and lipid metabolism.<sup>12</sup> mTORC2 was recently also shown to regulate size, shape, and synaptic plasticity of neurons<sup>13,14</sup> as well as oligodendrocyte differentiation.<sup>15</sup> These and other studies demonstrate that the functions of mTORC2 are diverse and specific for the tissue or cell type being analysed.

The mTORC1 inhibitor rapamycin is used as an immunosuppressant and an anticancer drug, and the interest to use it for ageing-related disease including cardiac disease is also high. Notably, rapamycin does not fully block mTORC1<sup>16</sup> and it was reported to activate mTORC2 and Akt, which may be anti-apoptotic.<sup>17</sup> On the other hand, long-term rapamycin treatment can also inhibit mTORC2.<sup>18,19</sup> Our present study therefore aims to uncover the cardiac function of rictor/mTORC2 using a conditional knockout approach. We report that deletion of *rictor* from cardiomyocytes inactivates mTORC2, but does not modify basal cardiac function and geometry during postnatal growth and up to an age of 54 weeks. However, rictor-deficient hearts perform less well when challenged by aortic constriction-induced pressure overload, despite the fact that their reactive hypertrophy is similar as in controls. Our data suggest that mTORC2 is implicated in the contractile response to pathological haemodynamic stress and further molecular analyses point to PKC $\beta$ II and PKC $\delta$  as effectors of mTORC2 in our model.

## 2. Methods

### 2.1 Animals

Male rictor knockout and control mice on a C57BL/6 background were generated using tamoxifen-inducible Cre-recombinase under control of the cardiomyocyte-specific  $\alpha$ -myosin heavy chain (MHC) promoter.<sup>7</sup> Transverse aortic constriction (TAC) and echocardiography were performed as published, using ketamine/xylazine and isoflurane, respectively.<sup>7</sup> Animal experiments were performed according to Guidelines for the Care and Use of Laboratory Animals and with approval of the Swiss Cantonal Authorities.

### 2.2 Cardiomyocyte isolation

Cardiomyocytes were isolated from control and cardiac rictor knockout (rictor-cKO) mice at 12 weeks of age as published.<sup>20</sup>

### 2.3 Protein and RNA analysis

Equal amounts of protein or RNA extracted from tissues and cultured cardiomyocytes were analysed by immunoblotting and quantitative real-time PCR as reported.<sup>7</sup>

### 2.4 Microscopic analysis

Paraffin sections of 4% paraformaldehyde-fixed tissue were processed for Picrosirius red staining to visualize fibrosis. Deoxynucleotidyl transferase dUTP nick end-labelling (TUNEL) assay was performed using an *in situ* apoptosis detection kit (Roche Diagnostics, Rotkreuz, Switzerland). Wheat germ agglutinin (WGA) staining, collagen, and caspase-3 labelling were done on cryosections fixed with 4% paraformaldehyde.<sup>7</sup> Cross-sectional areas were quantified by measuring at least 100 cardiomyocytes in three independent sections of 3–4 mice per group.

### 2.5 Statistical analysis

Data are presented as mean  $\pm$  SEM. Differences in means were evaluated with two-way ANOVA (*P*-values in text), followed by Sidak's multiple comparisons tests (*P*-values in figures). For multiple measurements of the same mice, repeated-measures ANOVA was used. All statistics was performed with GraphPad Prism 6.0. *P*-values of  $<0.05$  were considered statistically significant.

Detailed procedures, antibody sources, and buffer compositions are provided in Supplementary material online.

## 3. Results

### 3.1 Rictor deficiency does not affect cardiac weight, function, or geometry in adult mice up to 54 weeks of age or in growing young mice

To analyse the cardiac function of mTORC2, we generated cardiac-specific rictor knockout mice by crossing mice containing the floxed *rictor* gene<sup>9,21</sup> with mice transgenic for inducible Cre-recombinase driven by the  $\alpha$ -MHC promoter.<sup>22</sup> The resulting *rictor*<sup>fl/fl</sup>  $\alpha$ -MHC-MerCreMer<sup>Tg/0</sup> mice were, at an age of 10 weeks, injected with tamoxifen to induce the deletion. These mice are hereafter referred to as rictor-cKO mice. Control mice (*rictor*<sup>+/+</sup>  $\alpha$ -MHC-MerCreMer<sup>Tg/0</sup>) underwent the same tamoxifen treatment. 18 days after the tamoxifen injections, rictor protein was lower in the rictor-cKO mice compared with the control mice in cardiac muscle, but not in skeletal muscle. Moreover, insulin-stimulated increases in Akt-pS473 were dramatically impaired while 4E-BP1 phosphorylation was not affected in the rictor-cKO hearts (Figure 1A). This confirms specificity of the deletion and efficient inactivation of mTORC2, because Ser473 in the hydrophobic motif (HM) of Akt is the best-established direct target of mTORC2. At this time point after induction of the deletion, no cardiac functional or geometric differences were revealed by ultrasound analysis between the control and rictor-cKO mice. To evaluate the consequences of prolonged mTORC2 inactivation under basal conditions, we performed echocardiography at 4, 6, 10, 16, and 25 weeks after tamoxifen to assess cardiac parameters at 14, 16, 20, 26, and 35 weeks of age (see Supplementary material online, Figure S1A and Table S1). At all time points, the ejection fraction (EF) and fractional shortening (FS) values of the rictor-cKO mice were similar to those of control mice. Systolic and diastolic septum and left ventricular (LV) posterior wall thickness, LV internal diameters, and LV mass-to-body weight ratios were also indistinguishable over the time period that these mice were followed. Consistently, *post-mortem* analysis at the age of 35 weeks revealed no differences in ventricular weight to tibia length ratios between the control and rictor-cKO mice. In an independent experiment with a different batch of mice, we found that even at 54 weeks of age, rictor-cKO mice were indistinguishable from control mice (Table 1). Notably, at both 35 and 54 weeks, rictor protein and mTORC2 activity, as assessed by the amount of Akt-pS473,

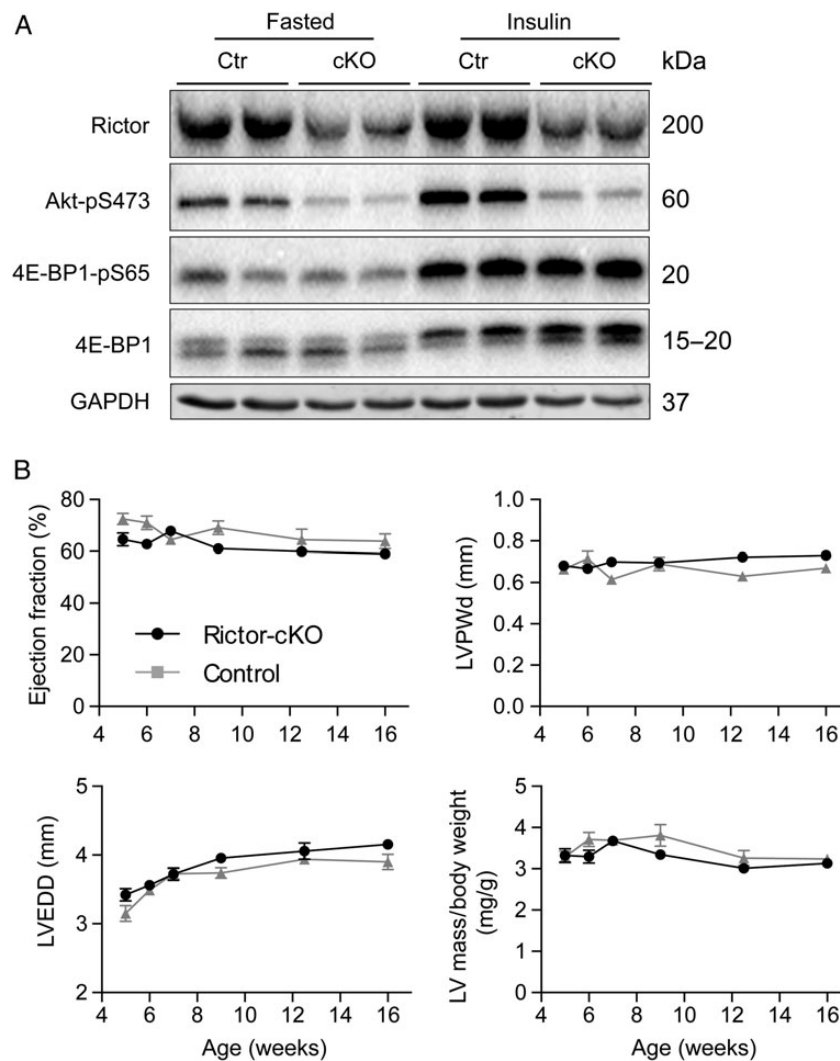


**Figure 1** Baseline characterization of rictor-deficient mice at 18 days after induction of the deletion (A), and analysis of the consequences of rictor deficiency in young growing mice (B). (A) At 18 days after tamoxifen, overnight-fasted male mice were stimulated with vehicle ('fasted') or insulin for 2 h, sacrificed, and the left ventricle was dissected and snap-frozen for analysis by western blotting with antibodies as indicated. (B) Ultrasound measurements of EF, diastolic LV posterior wall thickness (LVPWd), LVEDD, and LV mass-to-body weight ratios are shown at the indicated ages. *Rictor* deletion at 10 (A) and 4 (B) weeks of age. Rictor-cKO: tamoxifen-injected  $\alpha$ -MHC-MerCreMer/*rictor*<sup>fl/fl</sup> ( $N = 9$ ). Controls: tamoxifen-injected  $\alpha$ -MHC-MerCreMer/*rictor*<sup>+/+</sup> ( $N = 4$ ). Statistical analysis: repeated-measures ANOVA.

were still significantly decreased (see Supplementary material online, Figure S1B).

As mTOR and Akt have been implicated in growth regulatory mechanisms, we next deleted cardiac *rictor* in growing mice at 4 weeks of age. We observed a normal increase in LV mass over time with no differences between the rictor-cKO and control mice. Cardiac growth was in proportion to whole body growth for both groups, as LV mass-to-body weight ratios were identical over time (Figure 1B). Moreover, EFs and all other echocardiographic parameters were normal during growth and up to an age of 16 weeks (see Supplementary material online, Table S2). Thus, rictor deficiency does not affect physiological cardiac growth in young mice and has no adverse effects on cardiac function in healthy adult mice kept under laboratory conditions up to 54 weeks of age, the latest time point analysed in our study.

### 3.2 Rictor deficiency accelerates the development of cardiac dysfunction after aortic constriction

The above data show that despite significant changes in Akt phosphorylation at Ser473, rictor-cKO mice have a virtually normal functional cardiac phenotype. We reasoned that mTORC2 may primarily function as a modulator of cardiac function during cardiac stress and therefore assessed the effect of rictor deficiency in the cardiac response to pathological pressure overload induced by TAC. Rictor-cKO and control mice were assigned randomly to sham or TAC groups for surgery at 18 or 19 days after tamoxifen. Echocardiography was performed before (see Supplementary material online, Table S3) and 1 week after TAC (Figure 2A and Table 2). Prior to TAC, no differences were detectable between any of the experimental groups. In the control mice, 1

**Table 1** Echocardiographic parameters of control and rictor knockout mice at 54 weeks of age

	Control (N = 6)	Rictor-cKO (N = 5)
Echocardiography		
Heart rate (b.p.m.)	500 ± 28	563 ± 16
Anteroseptal wall thickness (mm)		
Diastole	0.97 ± 0.04	0.82 ± 0.07
Systole	1.36 ± 0.05	1.17 ± 0.11
LV wall thickness (mm)		
Diastole	0.75 ± 0.02	0.82 ± 0.04
Systole	1.05 ± 0.06	1.11 ± 0.07
LV internal diameter (mm)		
Diastole	4.11 ± 0.05	4.11 ± 0.2
Systole	2.88 ± 0.04	3.03 ± 0.24
Ejection fraction (%)	61.3 ± 1.4	55.9 ± 4.0
Fractional shortening (%)	32.6 ± 1.0	29.0 ± 2.7
Post-mortem analysis		
Body weight (g)	40.6 ± 1.6	39.8 ± 2.2
Ventricular weight (VW, mg)	123.2 ± 5.4	120.0 ± 5.9
VW/body weight (mg/mm)	3.05 ± 0.15	3.03 ± 0.09

Rictor deletion was induced in  $\alpha$ -MHC-MerCreMer/rictor<sup>fl/fl</sup> mice at the age of 10 weeks by an intraperitoneal injection with tamoxifen for 5 consecutive days. Controls consisted of mice homozygous for the wild-type rictor gene ( $\alpha$ -MHC-MerCreMer/rictor<sup>+/+</sup>), injected with tamoxifen. Ultrasound analysis was performed at 44 weeks after tamoxifen. N = 5 for rictor-cKO and N = 6 for control.

week of TAC significantly increased the LV posterior and anteroseptal wall thickness while not changing the LV end-systolic and end-diastolic internal diameters. Moreover, the control mice maintained cardiac function after TAC, as their EF and FS values were similar to those measured after sham surgery. In the rictor-cKO, however, TAC significantly reduced EF and FS compared with sham-operated rictor-cKO or TAC-operated control mice. The rictor-cKO mice had higher LV end-diastolic diameters (LVEDD), an effect that was strongest at the end of systole. Moreover, although after TAC the rictor-cKO mice displayed increases in anteroseptal and LV posterior wall thickness, these increases were less pronounced than those measured in control mice. Taken together, these data indicate that the rictor-cKO mice developed signs of eccentric LV hypertrophy with a decline in cardiac function, whereas control mice were in the compensatory phase of hypertrophy after 1 week of TAC.

### 3.3 Rictor deficiency does not affect hypertrophy, fibrosis, or metabolic gene expression after TAC

Post-mortem analysis at 1 week after TAC revealed that the ventricular weight to tibia length ratios were not different between control and rictor-cKO mice. Thus, both groups produced similar increases in cardiac weight compared with the corresponding sham-operated groups (Figure 2B). In line with an unaltered hypertrophic response, atrial natriuretic peptide (ANP) and brain natriuretic peptide (BNP) were induced similarly in both groups (Figure 2B and D). TAC also increased skeletal muscle actin and decreased  $\alpha$ -MHC mRNA levels but again, these changes happened irrespective of the absence or presence of rictor (Figure 2C). Notably,  $\beta$ -MHC mRNA transcript levels were higher in

the rictor-cKO mice than in controls under sham and TAC conditions (Figure 2C), although the effect did not reach statistical significance at the protein level (Figure 2D). WGA labelling (Figure 3A), Picrosirius red staining (Figure 3B), collagen I (Figure 3C) and collagen III immunolabelling (not shown), as well as gene expression analysis (Figure 3D and see Supplementary material online, Figure S2) showed that cardiomyocyte cross-sectional areas, fibrosis, and metabolic gene expression were not affected by the rictor deletion. Thus, after 1 week of pressure overload, the altered geometry and decreased function of the rictor-deficient hearts is not associated with any differences in cardiac weight, fibrosis, or hypertrophic and metabolic gene expression compared with the control mice.

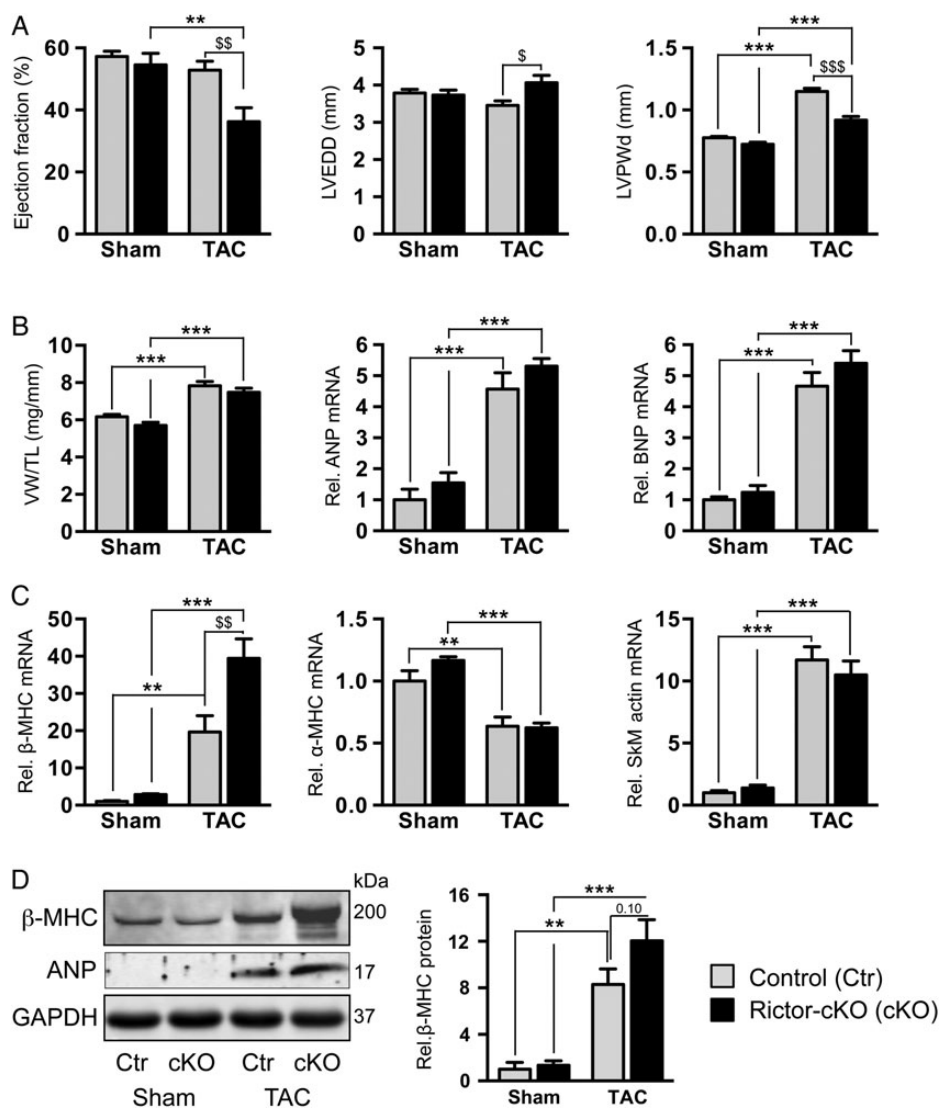
### 3.4 TAC increases rictor in control mice and rictor deficiency reduces protein levels of multiple PKC isoforms

Figure 4A shows that TAC caused a significant 1.65-fold increase in rictor protein in control mice, an observation that *per se* provides support for a role of rictor/mTORC2 in pressure-overload conditions. TAC also augmented rictor protein somewhat in the knockout mice ( $P = 0.12$ ), which is explained by the fact that the gene is not excised from all cardiac cells.<sup>22</sup> To obtain insights into the mechanisms whereby mTORC2 supports cardiac function during pressure overload, we proceeded to analyse the phosphorylation state of several AGC kinases, direct targets of mTORC2, in cardiac protein extracts. Since rictor deficiency did not modify the hypertrophic growth response to TAC, we directed our attention to the PKC family of kinases, which have been implicated in metabolism and contractility.<sup>23–25</sup> One of the classical PKCs (cPKC), namely PKC $\alpha$ , is a well-established direct target of mTORC2,<sup>26</sup> and recent work shows that several other PKCs may also be regulated by mTORC2.<sup>13</sup> Given their known importance in cardiac disease, we set out to analyse which of the PKC isoforms were regulated in our TAC model and to what extent rictor deficiency modified this regulation. Figure 4B shows that in control mice, TAC increased total protein levels of the classical PKC $\beta$ II as well as PKC $\delta$ , a novel PKC (nPKC) by 1.5- and 2.3-fold, respectively. For PKC $\beta$ II, the increase was paralleled by enhanced phosphorylation of its HM residue Ser660 (Figure 4B and see Supplementary material online, Figure S3A). An antibody to Thr638/641 in PKC $\alpha$ / $\beta$ II revealed that phosphorylation of this turn motif (TM) was also increased (Figure 4B). Probing with a PKC $\beta$ II-specific TM site antibody confirmed that this indeed concerned phosphorylation of the PKC $\beta$ II isoform and that the difference between control and rictor-cKO mice was already visible prior to surgery (see Supplementary material online, Figure S3B). As the above-mentioned phosphorylation sites are all typical mTORC2 targets and the increases in total and phosphorylated PKCs paralleled those observed for rictor shown in Figure 4A, we next assessed whether rictor/mTORC2 is required for their increased abundance under pressure-overload conditions. Indeed, the significant increases in PKC $\beta$ II and PKC $\delta$  protein were absent in the rictor-cKO hearts and consistently, PKC $\beta$ II-pS660 and -pT641 were lower in rictor-cKO than in control mice (Figure 4B).

While the rictor-cKO group had lower PKC $\alpha$  and - $\beta$ II levels compared with the control group, the abundance of PKC $\delta$  appeared not affected by rictor ablation under basal (sham) conditions (Figure 4B). We also analysed PKC $\epsilon$ , the other main nPKC expressed in the heart. Its protein levels were lower in the rictor-cKO than in the corresponding sham or TAC controls, and did not increase after TAC (Figure 4B and see Supplementary material online, Figure S3C).

In conclusion, our observation that TAC increases PKC $\beta$ II and PKC $\delta$  along with rictor in control, but not in the rictor-cKO hearts, suggests





**Figure 2** Rictor deficiency causes cardiac dysfunction without changing hypertrophic responses after TAC. Rictor deletion was induced by tamoxifen at 10 weeks of age and TAC or sham surgery performed 18–19 days later. Ultrasound was performed before (see Supplementary material online, Table S1) and 1 week after surgery (A), and the mice were sacrificed for molecular analysis immediately afterwards (B–D). (A) Echocardiography data of the EF, LVEDD, and diastolic LV posterior wall thickness (LVPWd). (B) Post-mortem ventricular weight to tibia length ratios (VW/TL) and quantitative RT-PCR analysis of ANP and BNP. (C) Quantitative RT-PCR analysis of  $\beta$ -MHC,  $\alpha$ -MHC, and skeletal muscle (SkM) actin mRNA levels. (D) Western analysis of ANP and  $\beta$ -MHC proteins. Rictor-cKO are tamoxifen-injected  $\alpha$ -MHC-MerCreMer/*rictor*<sup>fl/fl</sup> mice (N = 5 for sham, N = 7 for TAC). Controls are tamoxifen-injected  $\alpha$ -MHC-MerCreMer/*rictor*<sup>+/+</sup> mice (N = 6 for sham, N = 6 for TAC). Two-way ANOVA post hoc testing: \*\**P* < 0.01, \*\*\**P* < 0.001 for TAC vs. sham; \$*P* < 0.05, \$\$*P* < 0.01, \$\$\$*P* < 0.001 for rictor-cKO vs. control.

that the inability to increase these isozymes contributes to the reduced cardiac performance observed in our rictor-cKO mice under pressure-overload conditions. As PKC $\beta$ II was already affected under basal conditions, its decrease is likely implicated directly in the development of dysfunction. Although PKC $\epsilon$  was not increased after TAC, its strongly reduced levels in rictor-cKO hearts may have contributed to the dysfunction.

### 3.5 Rictor deficiency reduces Akt-pS473, Akt-pS450, as well as total Akt1 and 2 protein, while increasing Akt-pT308

Akt is the most frequently analysed target of mTORC2 and serves as an important survival kinase in the heart (for review, see Sussman *et al.*<sup>27</sup>).

Consistent with the baseline data obtained at 18 days after tamoxifen (Figure 1A) phosphorylation of Akt at its HM residue, Ser473 was also strongly reduced in the rictor-deficient hearts at 1 week after surgery, i.e. 25 days after tamoxifen, confirming that mTORC2 was to a large extent inactivated. Notably, total Akt protein was also lower in the rictor-cKO mice than in controls. Antibodies specific for total Akt1 and Akt2 protein (Figure 4C) revealed that both isoforms were reduced significantly. As previous studies have shown that mTORC2-mediated TM phosphorylation determines the stability and thereby abundance of Akt,<sup>28,29</sup> we analysed Akt-pS450. Figure 4C shows that phosphorylation of this site was indeed strongly diminished in the rictor-cKO hearts. Notably, Akt phosphorylation at Thr308, thought to be key for Akt activity,<sup>30</sup> was not reduced despite a clear lack of phosphorylation at

**Table 2** Physiological and echocardiographic parameters of control and rictor knockout mice at 1 week after sham or TAC surgery

	Control		Rictor-cKO	
	Sham (N = 7)	TAC (N = 6)	Sham (N = 5)	TAC (N = 7)
Echocardiography				
Heart rate (b.p.m.)	539 ± 25	495 ± 14	473 ± 16	514 ± 13
Anteroseptal wall thickness (mm)				
Diastole	0.77 ± 0.01	1.04 ± 0.02***	0.73 ± 0.02	0.89 ± 0.03***, \$\$\$
Systole	1.03 ± 0.02	1.39 ± 0.03***	0.97 ± 0.04	1.12 ± 0.04*, \$\$\$
LV posterior wall thickness (mm)				
Diastole	0.78 ± 0.01	1.15 ± 0.03***	0.72 ± 0.02	0.92 ± 0.03***, \$\$\$
Systole	1.03 ± 0.02	1.36 ± 0.03***	0.97 ± 0.04	1.07 ± 0.05*, \$\$\$
LV internal diameter (mm)				
Diastole	3.79 ± 0.10	3.46 ± 0.13	3.73 ± 0.13	4.06 ± 0.20 <sup>§</sup>
Systole	2.67 ± 0.10	2.55 ± 0.16	2.70 ± 0.18	3.38 ± 0.26 <sup>§§</sup>
Ejection fraction (%)	57.2 ± 1.7	52.8 ± 3.2	54.6 ± 3.7	36.2 ± 4.5**, \$\$\$
Fractional shortening (%)	29.6 ± 1.1	26.6 ± 2.0	27.9 ± 2.4	17.3 ± 2.3**, \$\$\$
Post-mortem analysis				
Body weight (g)	29.0 ± 0.4	26.6 ± 1.1**	26.9 ± 0.8	27.1 ± 0.7
Ventricular weight (VW, mg)	112.4 ± 2.0	143.7 ± 4.2***	103.9 ± 3.1	135.9 ± 4.1***
VW/tibial length (mg/mm)	6.17 ± 0.13	7.84 ± 0.24***	5.69 ± 0.18	7.49 ± 0.22***

\* $P < 0.05$ , \*\* $P < 0.01$ , \*\*\* $P < 0.001$ : TAC- vs. corresponding sham-operated group.

<sup>§</sup> $P < 0.05$ , <sup>§§</sup> $P < 0.01$ , <sup>§§§</sup> $P < 0.001$ : knockout vs. corresponding control group.

Ser473 and Ser450. Consistent with earlier studies,<sup>4,31</sup> Akt-pT308 appeared even somewhat higher in the rictor-cKO than in control mice ( $P = 0.035$  in two-way ANOVA), although upstream of Akt-pT308 no compensatory change in phosphoinositide-dependent kinase 1 (PDK1) phosphorylation was observed (see Supplementary material online, Figure S4A). In sham-operated mice, this went along with slightly enhanced phosphorylation of the Akt targets GSK3 $\beta$  and TSC2 (see Supplementary material online, Figure S4A). In an independent cohort of mice sacrificed at 18 days after tamoxifen in the fasted or insulin-stimulated state, rictor deficiency did not change phosphorylation of the Akt targets AS160 and FoxO1/3a (see Supplementary material online, Figure S4B). Our results are consistent with the view that Akt phosphorylation by mTORC2 is not required for its Thr308 phosphorylation by PDK1<sup>32</sup> and with what has been described for liver,<sup>12</sup> skeletal muscle,<sup>9</sup> Purkinje cells,<sup>13</sup> and other studies in which it was reported that Akt is still activated to a significant extent in mTORC2-deficient cells. Our findings show that also in the heart, the loss of mTORC2-mediated Akt phosphorylation does not reduce Akt activity towards several of its substrates.

### 3.6 Analysis of apoptosis in rictor-deficient hearts and adult cardiomyocyte cultures

Akt is known to propagate the effects of PI3K within the nucleus via FoxOs and thereby may regulate apoptosis.<sup>33,34</sup> Some studies support that mTORC2 is needed specifically for the function of Akt to phosphorylate FoxO, but not for other functions of Akt.<sup>35</sup> A recent study shows in cultured cardiomyocytes and ischaemic hearts that mTORC2 inactivation by Torin or shRNA enhances, whereas mTORC2 activation via PRAS40 decreases oxidative stress-induced apoptosis, and

suggests that this happens via Akt-pS473 and FoxO.<sup>36</sup> We therefore tested whether mTORC2 deficiency increased apoptosis in our model by analysing cleaved caspase-3 and performing TUNEL assays. After TAC, the rictor-cKO mice ( $N = 6$ ) had 2.2-fold more cleaved caspase-3-positive cells than the control mice ( $N = 5$ ) and consistently, they also contained more TUNEL-positive cells (Figure 5A and B). However, only very few apoptotic cells were detectable and these were all part of the non-cardiomyocyte compartment of the heart as identified by double labelling with antibodies to myomesin. Our finding that cardiomyocyte apoptosis was not detectable in sections of the whole heart was in apparent contrast with previous work,<sup>36</sup> and we therefore went on to analyse apoptosis by western blotting after isolation of cardiomyocytes from the adult control and rictor-cKO hearts. Figure 5C shows that rictor was below detection levels in this cardiomyocyte fraction of the heart, which confirms efficiency and cardiomyocyte specificity of the deletion. Cleaved caspase-3 was higher in rictor-depleted cardiomyocytes immediately (0 h) or 24 h after their isolation. These data show that mTORC2 prevents apoptosis in adult cardiomyocytes, at least during the isolation procedure of these cells, which is very likely associated with hypoxic and/or other stress. Nevertheless, our observation that overall cardiac weight, fibrosis, and cardiomyocyte cross-sectional areas were not changed by the deletion together with the fact that we did not detect any apoptotic cardiomyocytes in the *in situ* heart indicates that apoptosis is not a primary reason for the dysfunction measured in rictor-deficient pressure-overloaded hearts. This conclusion is further supported by our observation that phosphorylated FoxO1/3 was not altered by the *rictor* deletion (see Supplementary material online, Figure S4B) and consistently, multiple FoxO target genes (ERR $\alpha$ , MCD1, and CPT1b) were indistinguishable between control and rictor-cKO hearts (data not shown).

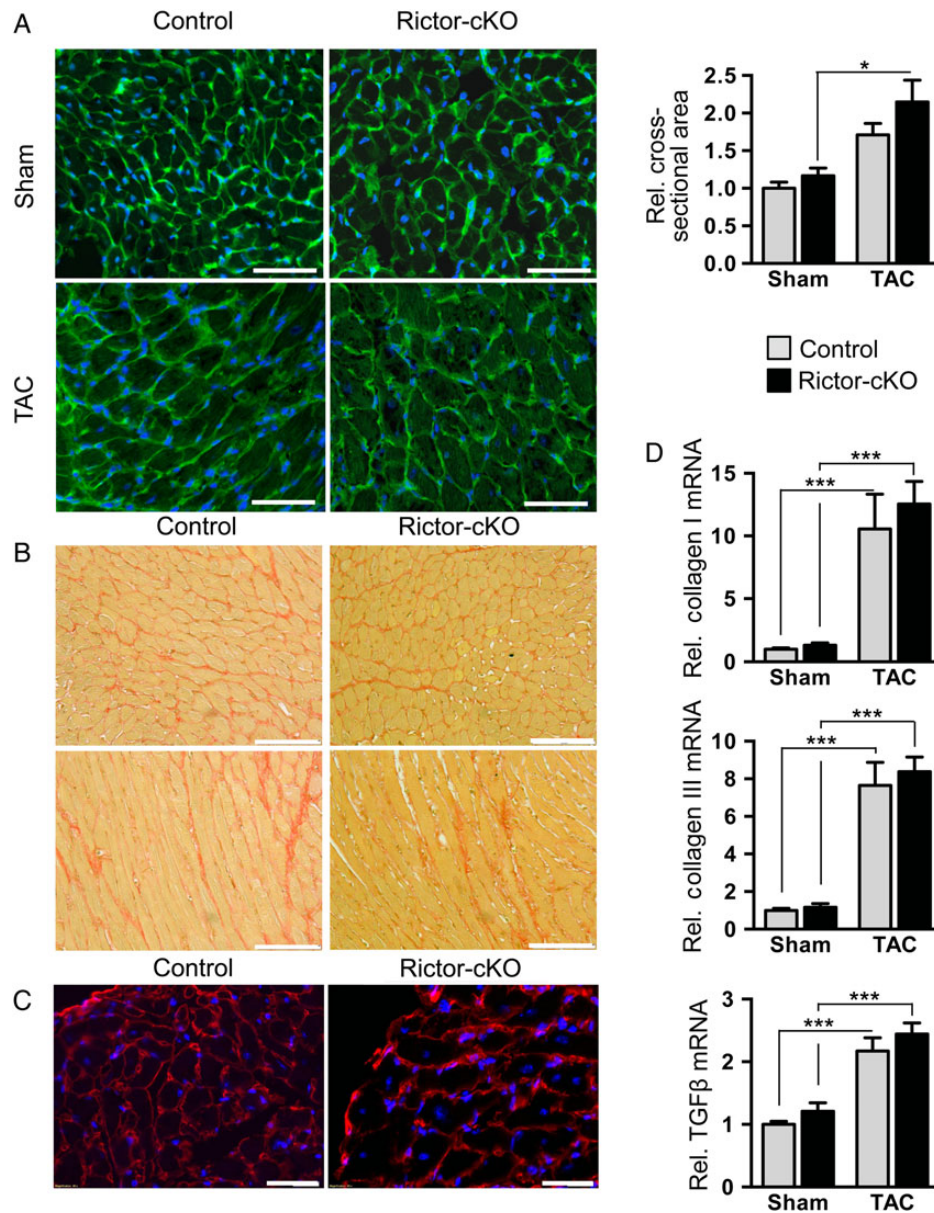


**Figure 3** Rictor deficiency does not change cardiomyocyte cross-sectional areas or fibrosis after aortic constriction. Cardiac tissue of mice of *Figure 2* was either frozen in OCT (A and C) or fixed in paraformaldehyde, followed by dehydration and embedding in paraffin (B), or snap-frozen in liquid nitrogen for isolation of RNA and quantitative RT-PCR analysis (D). (A) WGA staining (left) and quantitative analysis of the cardiomyocyte cross-sectional area (right). (B) Picosirius red staining for analysis of fibrosis. (C) Immunolabelling with an antibody to collagen I followed by a rhodamine-labelled secondary antibody. (B and C) TAC-operated mice. (D) Quantitative RT-PCR of collagen I and III and transforming growth factor (TGF) $\beta$  to evaluate fibrosis ( $N = 5-6$  mice per group). Two-way ANOVA *post hoc* testing:  $*P < 0.05$ ;  $***P < 0.001$  for TAC vs. the corresponding sham control. The scale bars represent 100  $\mu\text{m}$ .

### 3.7 Rictor deficiency blunts signalling via PRAS40, mTORC1, and rpS6

Next to the Akt targets GSK3 $\beta$ , TSC2, and AS160 described under Section 3.5, reduced Akt levels in rictor-deficient hearts could, via PRAS40 and TSC, diminish mTORC1 activity. Since changed signalling via mTORC1 may, at least in part, explain the functional phenotype of the rictor-cKO mice, we tested whether mTORC2 inactivation modified signalling via mTORC1. Whereas *Figure 6A* shows that phosphorylation of the mTORC1 targets 4E-BP1 and

UNC-51-like kinase 1 (ULK1) were not affected by *rictor* ablation, *Figure 6B* shows a trend towards lower S6-pS240/244 in rictor-deficient hearts ( $P = 0.068$  in two-way ANOVA), suggesting reduced signalling via mTORC1/p70-S6K1. Consistently, mTOR phosphorylation at Ser2448, a target of p70-S6K1 indicative of mTORC1 activation, was decreased after *rictor* deletion ( $P = 0.006$  in two-way ANOVA, *Figure 6B*). Furthermore, PRAS40, a target of Akt and component and negative regulator of mTORC1, was less phosphorylated in the rictor-cKO mice ( $P = 0.011$  in two-way ANOVA, *Figure 6B*). Our findings suggest that mTORC2 may, possibly via Akt and

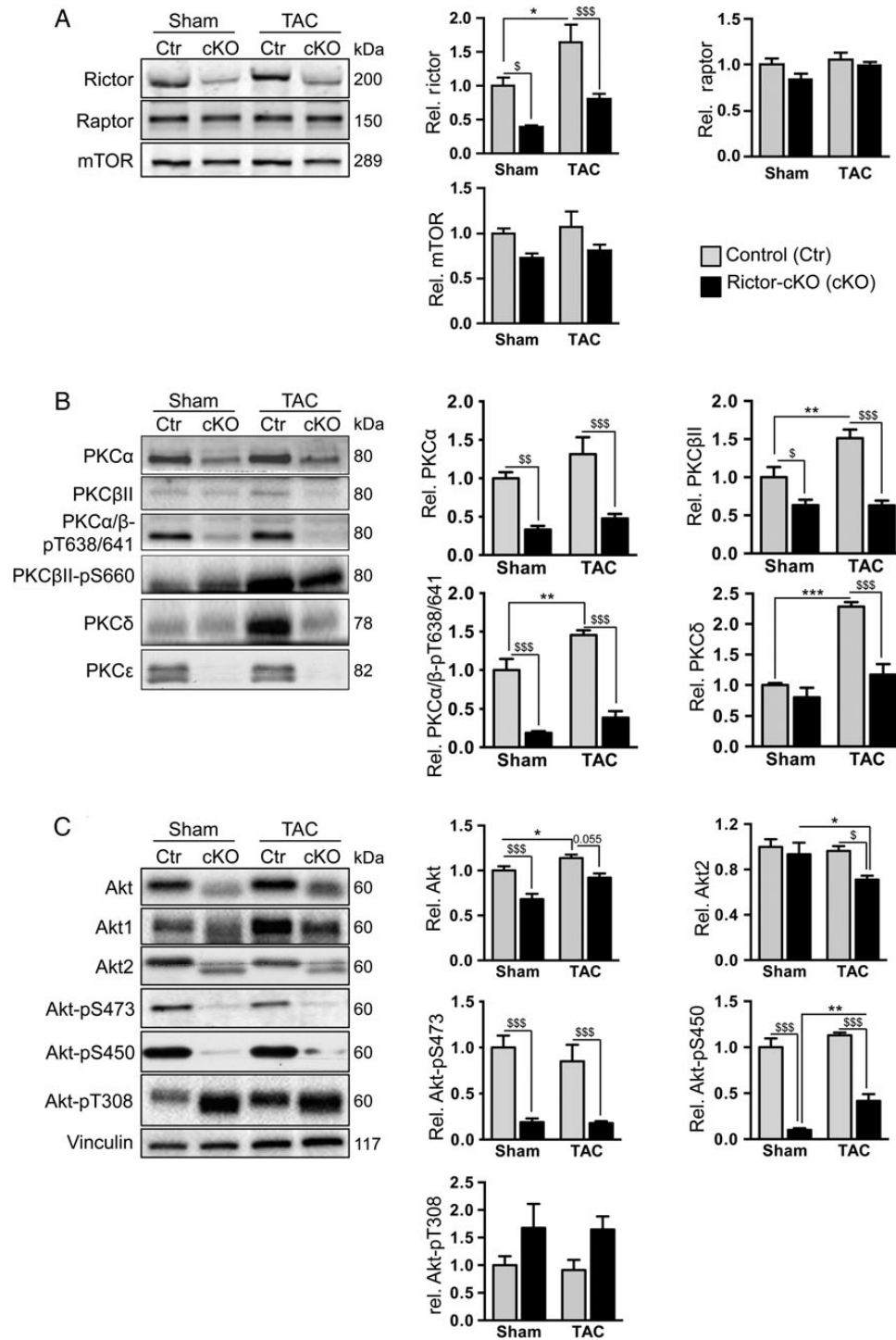


**Figure 4** Effects of TAC and *rictor* ablation on AGC signalling at 1 week after surgery. Examples of western blots incubated with the antibodies as indicated (left). Quantification after normalization to the corresponding loading controls (right). The normalized data are expressed relative to the sham-operated controls. Control and rictor-cKO mice as in Figure 2.  $N = 5-7$  per group. Two-way ANOVA *post hoc* testing: \* $P < 0.05$ , \*\* $P < 0.01$ , \*\*\* $P < 0.001$  for TAC vs. sham;  $^{\$}P < 0.05$ ,  $^{\$\$}P < 0.01$ ,  $^{\$\$\$}P < 0.001$  for rictor-cKO vs. control.

PRAS40, regulate mTORC1-mediated p70-S6K1 and rpS6 phosphorylation. We also analysed AMPK $\alpha$ , as it is known to independently repress mTORC1 signalling through specific phosphorylation sites on mTOR, raptor, and TSC2 (reviewed in Shimobayashi and Hall<sup>37</sup>). AMPK $\alpha$  phosphorylation was increased in the rictor-deficient hearts ( $P = 0.012$  in two-way ANOVA). Thus, AMPK may have blocked

mTORC1 activity towards p70-S6K1 in parallel to PRAS40. Notably, the observed increase in AMPK $\alpha$  phosphorylation is indicative of increased AMP/ATP ratios, suggesting that energy availability is decreased in the rictor-cKO hearts. Indicative of metabolic stress is also the observed induction of  $\beta$ -MHC gene expression in the rictor-deficient mice (Figure 2).



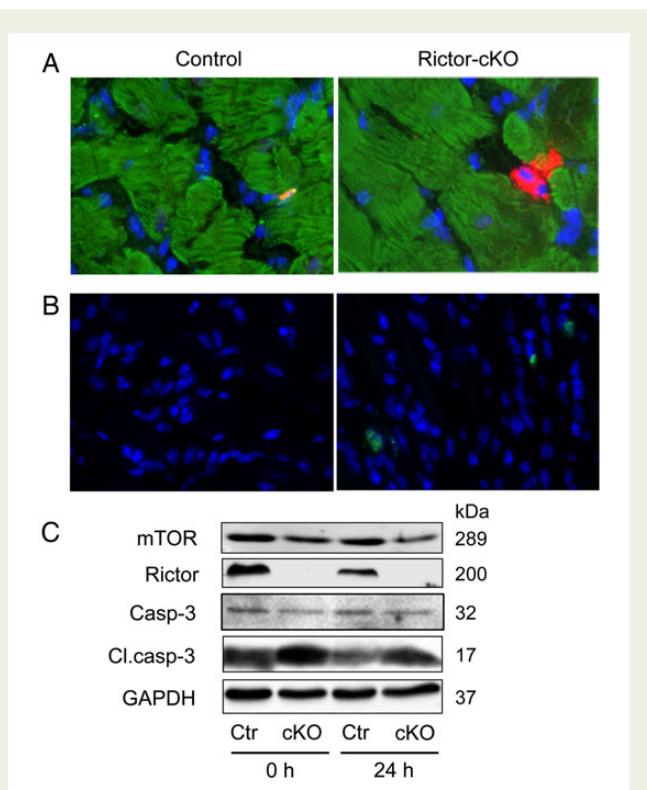


**Figure 5** mTORC2 inactivation increases apoptosis in non-myocyte cells of the heart. Cardiac tissue of the mice of Figure 2 was frozen in OCT (A) or fixed in paraformaldehyde, followed by dehydration and embedding in paraffin (B). (A) Immunostaining with an antibody against cleaved caspase-3 fragment followed by an Alexa555-labeled secondary antibody. Double labelling of the same section with an antibody to myomesin followed by an Alexa488-labelled antibody was performed to identify cardiomyocytes. (B) TUNEL assay was performed on paraffin sections. (A and B) Nuclei were stained with DAPI. For C, primary cardiomyocyte cultures were prepared from adult control and rictor cardiac knockout (cKO) mice and proteins extracted immediately (0 h) or 1 day after the isolation (24 h). Caspase-3 was analysed by western blotting.

## 4. Discussion

### 4.1 Rictor/mTORC2 is implicated in the response to pressure overload

The main objective of the present study was to elucidate the function of mTORC2 in the heart. Our experiments demonstrate that haemodynamic stress causes cardiac dysfunction in mice deficient for rictor, an essential component of mTORC2, whereas control mice with normal mTORC2 activity display maintained function. Cardiac mTORC2 inactivation does not cause any obvious basal phenotype during post-natal growth or adulthood up to 54 weeks of age. Interestingly, TAC increased overall ventricular weight in the rictor-cKO mice as much as in the control mice, but increases in LV wall thickness were less pronounced and associated with increased LV internal diameters, reminiscent of eccentric hypertrophy. Rictor deficiency did not affect any of the TAC-induced hypertrophic markers ANP, BNP, smooth muscle actin, and skeletal muscle actin, nor did it modify metabolic gene expression or fibrosis. Taken together, our results indicate that mTORC2 is

important for contractile performance in acute pressure-overload conditions, without affecting reactive hypertrophic responses.

### 4.2 Rictor/mTORC2 is required for increased PKC $\beta$ II and PKC $\delta$ protein levels during pressure overload

The role of mTORC2 during haemodynamic stress is further supported by our observation that rictor protein levels increase concomitant with maintained function in pressure-overloaded control hearts. This increase is paralleled by enhanced phosphorylation of PKC $\alpha$  and PKC $\beta$ II. Because mTORC2 has been implicated in the phosphorylation of multiple PKC family members,<sup>13,26,28,38,39</sup> our results suggest that cardiac mTORC2 participates in the response to haemodynamic stress via these effectors. The reduced phosphorylated levels of these PKCs after cardiac rictor ablation consolidate this view.

Total protein levels of PKC $\beta$ II, PKC $\delta$ , and, albeit to a lesser extent, PKC $\alpha$  ( $P = 0.16$ ) are also higher after TAC in control hearts, but not in rictor-deficient hearts. Consistent with earlier work in murine embryonic fibroblasts, where evidence was provided that co-translational TM site phosphorylation by mTORC2 regulates stability and thereby the abundance of PKC $\alpha$ ,<sup>27,39</sup> we here show that enhanced TM phosphorylation of PKC $\alpha$  and PKC $\beta$ II after TAC is associated with their increased abundance, whereas decreased phosphorylation of the same sites after rictor deletion is associated with their reduced abundance. Notably, the decrease in phosphorylated PKC was stronger than that in total PKC, indicating that the remaining protein was less phosphorylated. Similarly, the strongly reduced Akt and PKC $\epsilon$  abundance in our rictor-deficient hearts is very likely related to reduced mTORC2 phosphorylation, in line with previous mechanistic studies.<sup>13,28</sup> On the other hand, mTORC2 did not appear to regulate PKC $\delta$  in MEFs<sup>28,39</sup> or neurons,<sup>13</sup> and earlier work demonstrated TM autophosphorylation of PKC $\delta$ .<sup>40,41</sup> Our data therefore suggest that PKC $\delta$  stability may be regulated in a cell type-specific manner. It remains to be proven whether the decrease in PKC $\delta$  is explained by a direct mTORC2-mediated mechanism because unlike Akt and other PKCs that we measured, PKC $\delta$  appeared not reduced under basal conditions. We therefore cannot exclude the possibility that decreased PKC $\delta$  abundance after TAC is secondary to, for example, the observed cardiac or metabolic stress. Speaking against this is that cardiac stress has previously been associated with increased rather than decreased PKC $\delta$ . Alternatively, mTORC2-mediated PKC $\epsilon$  reductions could be responsible for the lowered PKC $\delta$ , as published previously,<sup>42</sup> because PKC $\epsilon$  is an established direct mTORC2 target.<sup>26,28,39</sup>

### 4.3 Functional consequences of reduced PKC $\beta$ II and PKC $\delta$ after TAC

Phosphorylation of the three conserved serine/threonine residues on cPKCs and nPKCs takes place shortly after synthesis and is needed for their intracellular distribution, stability, and catalytic activity.<sup>43,44</sup> These phosphorylation events cause a stable but still 'closed' inactive enzyme conformation and prepare them for subsequent activation by lipid second messengers, such as diacylglycerol (DAG) and Ca<sup>2+</sup>. In pressure-overload models, stimulation of angiotensin AT<sub>1</sub> and  $\alpha_1$ -adrenergic receptors will, via Gq and DAG, stimulate the PKCs. Increased PKC expression and activity was previously thought to cause the pathological hypertrophy together with ERK1/2 and p38 stress-activated kinases. However, consistent with our observation that decreased levels of two cPKCs were not associated with any

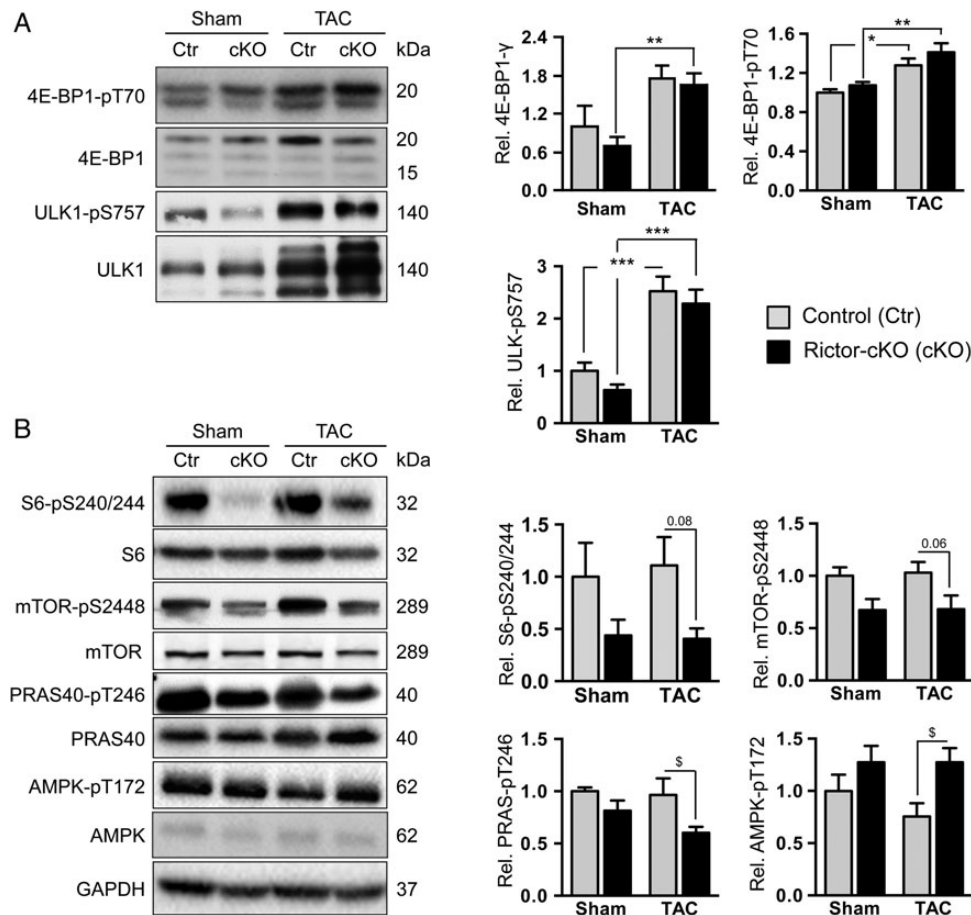


**Figure 6** Effect of *rictor* deletion on mTORC1, PRAS40, and AMPK. Examples of western blots incubated with antibodies as indicated (left). Quantification after normalization to the corresponding loading controls (right). The normalized data are expressed relative to the sham-operated controls. Control and rictor-cKO mice as in Figures 2 and 4.  $N = 5-7$  per group. Two-way ANOVA *post hoc* testing: \* $P < 0.05$ , \*\* $P < 0.01$ , \*\*\* $P < 0.001$  for TAC vs. sham;  $^{\$}P < 0.05$  for rictor-cKO vs. control.

effects on the hypertrophic response, genetic ablation of the cPKC family members does not prevent cardiac hypertrophy.<sup>45</sup> Instead, the cPKCs are today thought to be involved in the regulation of cardiac contractility.<sup>23</sup> Studies with PKC knockout mice have demonstrated that the  $\beta$  and  $\gamma$  isoforms are, in contrast to PKC $\alpha$ , positively affecting contractility. Thus, PKC $\beta/\gamma$  null mice show more severe failure, whereas PKC $\alpha$  null mice are less susceptible to heart failure following long-term pressure-overload or myocardial infarction injury.<sup>45</sup> Based on these studies, we think that our phenotype is related to the inability of the rictor-deficient hearts to increase PKC $\beta$ II and perhaps also PKC $\gamma$ , which we did not test in the heart but was strongly decreased after *rictor* ablation in neuronal tissue.<sup>13</sup>

Regarding the nPKCs, a study published during the revision of our manuscript demonstrated that PKC $\delta$  and PKC $\epsilon$  depress reactive hypertrophy, but that it required deletion of both genes to reveal this function, because redundancy masked the effect after ablation of the individual genes. The lack of a phenotype under basal conditions in our study with both nPKCs being strongly decreased after *rictor* ablation is consistent with that study, in which combined embryonic ablation of PKC $\delta$  and PKC $\epsilon$  showed no phenotype under basal conditions.<sup>35</sup> The lack of a significant effect on pressure-overload hypertrophy in the rictor-deficient mice may be due to residual PKC $\delta$  and

PKC $\epsilon$  protein, inherent to the inducible MerCreMer model that we used.

Besides contractile deficiency, the decreased cardiac performance may be related to the energy resources available for contraction, as mTORC2 has been implicated in the regulation of metabolism in various tissues.<sup>37,46</sup> In support of this idea, AMPK phosphorylation levels were increased in the rictor-cKO hearts indicative of a reduced ATP availability. Moreover,  $\beta$ -MHC expression was induced, which, as this isoform generates force in an energetically more economic manner than the  $\alpha$ -isoform, may represent a compensatory energy-preserving effort after *rictor* ablation. Akt2 regulates Glut4 translocation to the sarcolemma, a process that is enhanced during the cardiac pressure-overload response to ensure that energy supplies match the increased work. However, although Akt2 abundance was strongly reduced in the rictor-cKO hearts, the phosphorylation of its downstream mediator AS160 was not affected (see Supplementary material online, Figure S4B). Finally, the lack of a robust PKC $\delta$  increase after TAC, possibly secondary to decreased PKC $\epsilon$ ,<sup>42</sup> may explain metabolic insufficiency after *rictor* ablation, because it has been shown previously that hearts lacking PKC $\delta$  lose their capacity to adapt metabolically.<sup>47,48</sup> In conclusion, our data suggest that the lacking increases in PKC $\beta$ II and

PKC $\delta$  contributed to the dysfunction observed after pressure overload for the rictor-deficient hearts.

#### 4.4 Reduced phosphorylation of Akt at Ser473 and Ser450 after rictor ablation does not reduce Akt substrate phosphorylation

Next to the above-discussed PKCs, the protein abundance of the best-established mTORC2 target Akt was reduced in the rictor-cKO mice and this applies to Akt1 as well as Akt2. Because Akt was not increased in our TAC model, its reduced expression is most likely not a primary cause of the dysfunction measured in the rictor-cKO mice. The lack of a functional or morphological phenotype under physiological conditions in growing and adult mice suggests that the residual protein amounts were sufficient for normal cardiac function or that a high level of redundancy in cardiac signalling exists and alternate pathways compensate for the deletion. The latter possibility is supported by the fact that phosphorylation of Akt at Thr308 was not impaired and that the Akt targets GSK3 $\beta$ , TSC, and AS160 mirrored the Akt-pT308 levels, indicating normal Akt activity under basal conditions. These results imply that the mTORC2-mediated Akt phosphorylation is not essential for basal cardiac function. Consistently, cardiac deletion of mTOR<sup>4</sup> caused a basal phenotype that was very similar to that of mice in which raptor was lacking,<sup>7</sup> which indicates that mTOR acts predominantly as part of mTORC1. Similar observations were noted for other organs, including skeletal muscle,<sup>9,10</sup> kidney,<sup>49</sup> or adipose tissue<sup>11</sup> in all of which rictor deficiency does not cause any strong baseline phenotype. Along similar lines, mTORC2-mediated HM site phosphorylation appears not essential for the growth regulatory activity of Akt at physiological levels of insulin stimulation.<sup>50</sup> The latter study suggests that only the maximal levels of Akt activity are limited in the absence of HM phosphorylation, for example, when insulin stimulation is increased.<sup>50</sup> In analogy, our data obtained with the TAC model suggest that in the heart, the mTORC2-mediated phosphorylation becomes functionally important when mTORC2 targets are significantly activated, which we demonstrated for PKC $\beta$ II and PKC $\delta$ , but not for Akt. It is of note that our study was performed with male mice. Given the known effect of female hormones on Akt signalling, it remains to be demonstrated whether mTORC2 deficiency impacts one or more targets of Akt in the female heart.

#### 4.5 mTORC2 inactivation does not modify physiological or pathological cardiac growth

Our previous work shows that mTORC1 is essential for the cardiac adaptation to pressure overload with protein synthesis inherent to cardiomyocyte hypertrophy being one of the prior mechanisms implicated.<sup>7</sup> Upstream of mTORC1 and downstream of mTORC2 Akt can activate protein translation via TSC1/TSC2 and Rheb. Akt regulates normal postnatal cardiac growth,<sup>51</sup> it may get activated by pressure overload,<sup>52</sup> and transgenic overexpression of active Akt1 induces cardiac hypertrophy.<sup>53,54</sup> Whether or not mTORC2, via Akt or other pathways, contributes to cardiac growth responses was unclear at the onset of our study. As rictor deletion neither affected cardiac weight and cardiomyocyte cross-sectional areas after TAC, nor changed physiological postnatal cardiac growth, we conclude that mTORC2 is not required for cardiac protein synthesis. This is further supported by our observation that 4E-BP1, main mediator of protein synthesis downstream of mTORC1, was increased after TAC in the rictor-cKO as much as in control mice. Moreover, Akt-pT308 was increased along

with enhanced phosphorylation of targets involved in growth responses, such as TSC2 and GSK3 $\beta$ . In contrast, rictor ablation decreased S6K1 phosphorylation. While this effect may be secondary to decreased PKC activity,<sup>41,41,55,56</sup> it had no consequences for cardiac weight or cardiomyocyte cross-sectional area in our model, consistent with earlier work.<sup>57</sup> Thus, the heart behaves like several other organs from which rictor has been removed without affecting an increase in organ weight, including skeletal muscle,<sup>9,10</sup> adipose tissue,<sup>11</sup> and kidney.<sup>49</sup> We conclude that increased global protein synthesis intrinsic to physiological growth or pathological cardiac hypertrophy does not depend on mTORC2.

Taken together, our study points to a beneficial function of mTORC2 in the heart during haemodynamic stress. We identified several kinases that were reduced in rictor-deficient hearts. As cardiac dysfunction occurred only after haemodynamic stress, we conclude that the kinases that were increased concomitant to rictor in control but not in rictor-cKO hearts, namely PKC $\beta$ II and - $\delta$ , are implicated in the beneficial effects of mTORC2. As several compounds inhibiting both mTOR complexes are in clinical trials for the treatment of cancer, special attention should be paid in these studies to patients with concurrent cardiovascular diseases such as hypertension or valve disease. On the other hand, our insights into cardiac mTORC2 signalling may also open new avenues for the treatment of cardiac disease.

## Supplementary material

Supplementary material is available at *Cardiovascular Research* online.

**Conflict of interest:** none declared.

## Funding

This work was supported by the Swiss National Science Foundation (grant no. 31-135559/1), the 'Stiftung für Kardiovaskuläre Forschung Basel', and the 'Novartis Foundation for Medical-Biological Research'.

## References

- Sciarretta S, Volpe M, Sadoshima J. Mammalian target of rapamycin signaling in cardiac physiology and disease. *Circ Res* 2014;**114**:549–564.
- Dibble CC, Manning BD. Signal integration by mTORC1 coordinates nutrient input with biosynthetic output. *Nat Cell Biol* 2013;**15**:555–564.
- Song X, Kusakari Y, Xiao CY, Kinsella SD, Rosenberg MA, Scherrer-Crosbie M, Hara K, Rosenzweig A, Matsui T. mTOR attenuates the inflammatory response in cardiomyocytes and prevents cardiac dysfunction in pathological hypertrophy. *Am J Physiol Cell Physiol* 2010;**299**:C1256–C1266.
- Zhang D, Contu R, Latronico MV, Zhang JL, Rizzi R, Catalucci D, Miyamoto S, Huang K, Ceci M, Gu Y, Dalton ND, Peterson KL, Guan KL, Brown JH, Chen J, Sonenberg N, Condorelli G. mTORC1 regulates cardiac function and myocyte survival through 4E-BP1 inhibition in mice. *J Clin Invest* 2010;**120**:2805–2816.
- Wullschlegel S, Loewith R, Hall MN. TOR signaling in growth and metabolism. *Cell* 2006;**124**:471–484.
- Laplante M, Sabatini DM. mTOR signaling in growth control and disease. *Cell* 2012;**149**:274–293.
- Shende P, Plaisance I, Morandi C, Pellieux C, Berthonneche C, Zorzato F, Krishnan J, Lerch R, Hall MN, Ruegg MA, Pedrazzini T, Brink M. Cardiac raptor ablation impairs adaptive hypertrophy, alters metabolic gene expression, and causes heart failure in mice. *Circulation* 2011;**123**:1073–1082.
- Oh WJ, Jacinto E. mTOR complex 2 signaling and functions. *Cell Cycle* 2011;**10**:2305–2316.
- Bentzinger CF, Romanino K, Cloetta D, Lin S, Mascarenhas JB, Oliveri F, Xia J, Casanova E, Costa CF, Brink M, Zorzato F, Hall MN, Ruegg MA. Skeletal muscle-specific ablation of raptor, but not of rictor, causes metabolic changes and results in muscle dystrophy. *Cell Metab* 2008;**8**:411–424.
- Kumar A, Harris TE, Keller SR, Choi KM, Magnuson MA, Lawrence JC Jr. Muscle-specific deletion of rictor impairs insulin-stimulated glucose transport and enhances basal glycogen synthase activity. *Mol Cell Biol* 2008;**28**:61–70.
- Cybulski N, Polak P, Auwerx J, Ruegg MA, Hall MN. mTOR complex 2 in adipose tissue negatively controls whole-body growth. *Proc Natl Acad Sci USA* 2009;**106**:9902–9907.



12. Hagiwara A, Cornu M, Cybulski N, Polak P, Betz C, Trapani F, Terracciano L, Heim MH, Ruegg MA, Hall MN. Hepatic mTORC2 activates glycolysis and lipogenesis through Akt, glucokinase, and SREBP1c. *Cell Metab* 2012;**15**:725–738.
13. Thomanetz V, Angliker N, Cloetta D, Lustenberger RM, Schweighauser M, Oliveri F, Suzuki N, Ruegg MA. Ablation of the mTORC2 component rictor in brain or Purkinje cells affects size and neuron morphology. *J Cell Biol* 2013;**201**:293–308.
14. Huang W, Zhu PJ, Zhang S, Zhou H, Stoica L, Galiano M, Krnjevic K, Roman G, Costa-Mattioli M. mTORC2 controls actin polymerization required for consolidation of long-term memory. *Nat Neurosci* 2013;**16**:441–448.
15. Bercury KK, Dai J, Sachs HH, Ahrendsen JT, Wood TL, Macklin WB. Conditional ablation of raptor or rictor has differential impact on oligodendrocyte differentiation and CNS myelination. *J Neurosci* 2014;**34**:4466–4480.
16. Choo AY, Yoon SO, Kim SG, Roux PP, Blenis J. Rapamycin differentially inhibits S6Ks and 4E-BP1 to mediate cell-type-specific repression of mRNA translation. *Proc Natl Acad Sci USA* 2008;**105**:17414–17419.
17. Wang X, Yue P, Kim YA, Fu H, Khuri FR, Sun SY. Enhancing mammalian target of rapamycin (mTOR)-targeted cancer therapy by preventing mTOR/raptor inhibition-initiated, mTOR/rictor-independent Akt activation. *Cancer Res* 2008;**68**:7409–7418.
18. Sarbassov DD, Ali SM, Sengupta S, Sheen JH, Hsu PP, Bagley AF, Markhard AL, Sabatini DM. Prolonged rapamycin treatment inhibits mTORC2 assembly and Akt/PKB. *Mol Cell* 2006;**22**:159–168.
19. Lamming DW, Ye L, Katajisto P, Goncalves MD, Saitoh M, Stevens DM, Davis JG, Salmon AB, Richardson A, Ahima RS, Guertin DA, Sabatini DM, Baur JA. Rapamycin-induced insulin resistance is mediated by mTORC2 loss and uncoupled from longevity. *Science* 2012;**335**:1638–1643.
20. Nagata K, Liao R, Eberli FR, Satoh N, Chevalier B, Apstein CS, Suter TM. Early changes in excitation-contraction coupling: transition from compensated hypertrophy to failure in Dahl salt-sensitive rat myocytes. *Cardiovasc Res* 1998;**37**:467–477.
21. Polak P, Cybulski N, Feige JN, Auwerx J, Ruegg MA, Hall MN. Adipose-specific knock-out of raptor results in lean mice with enhanced mitochondrial respiration. *Cell Metab* 2008;**8**:399–410.
22. Sohal DS, Nghiem M, Crackower MA, Witt SA, Kimball TR, Tymitz KM, Penninger JM, Molkentin JD. Temporally regulated and tissue-specific gene manipulations in the adult and embryonic heart using a tamoxifen-inducible Cre protein. *Circ Res* 2001;**89**:20–25.
23. Liu Q, Molkentin JD. Protein kinase C alpha as a heart failure therapeutic target. *J Mol Cell Cardiol* 2011;**51**:474–478.
24. Palaniyandi SS, Sun L, Ferreira JC, Mochly-Rosen D. Protein kinase C in heart failure: a therapeutic target? *Cardiovasc Res* 2009;**82**:229–239.
25. Duquesnes N, Lezoualc'h F, Crozatier B. PKC-delta and PKC-epsilon: foes of the same family or strangers? *J Mol Cell Cardiol* 2011;**51**:665–673.
26. Guertin DA, Stevens DM, Thoreen CC, Burds AA, Kalaany NY, Moffat J, Brown M, Fitzgerald KJ, Sabatini DM. Ablation in mice of the mTORC components raptor, rictor, or mLST8 reveals that mTORC2 is required for signaling to Akt-FOXO and PKCalpha, but not S6K1. *Dev Cell* 2006;**11**:859–871.
27. Sussman MA, Volkens M, Fischer K, Bailey B, Cottage CT, Din S, Gude N, Avitabile D, Alvarez R, Sundaraman B, Quijada P, Mason M, Konstandin MH, Malhowski A, Cheng Z, Khan M, McGregor M. Myocardial AKT: the omnipresent nexus. *Physiol Rev* 2011;**91**:1023–1070.
28. Ikenoue T, Inoki K, Yang Q, Zhou X, Guan KL. Essential function of TORC2 in PKC and Akt turn motif phosphorylation, maturation and signalling. *EMBO J* 2008;**27**:1919–1931.
29. Oh WJ, Wu CC, Kim SJ, Facchinetti V, Julien LA, Finlan M, Roux PP, Su B, Jacinto E. mTORC2 can associate with ribosomes to promote cotranslational phosphorylation and stability of nascent Akt polypeptide. *EMBO J* 2010;**29**:3939–3951.
30. Alessi DR, James SR, Downes CP, Holmes AB, Gaffney PR, Reese CB, Cohen P. Characterization of a 3-phosphoinositide-dependent protein kinase which phosphorylates and activates protein kinase B alpha. *Curr Biol* 1997;**7**:261–269.
31. Zhu Y, Soto J, Anderson B, Riehle C, Zhang YC, Wende AR, Jones D, McClain DA, Abel ED. Regulation of fatty acid metabolism by mTOR in adult murine hearts occurs independently of changes in PGC-1alpha. *Am J Physiol Heart Circ Physiol* 2013;**305**:H41–H51.
32. Garcia-Martinez JM, Alessi DR. mTOR complex 2 (mTORC2) controls hydrophobic motif phosphorylation and activation of serum- and glucocorticoid-induced protein kinase 1 (SGK1). *Biochem J* 2008;**416**:375–385.
33. Brunet A, Park J, Tran H, Hu LS, Hemmings BA, Greenberg ME. Protein kinase SGK mediates survival signals by phosphorylating the forkhead transcription factor FKHRL1 (FOXO3a). *Mol Cell Biol* 2001;**21**:952–965.
34. Aoyama T, Matsui T, Novikov M, Park J, Hemmings B, Rosenzweig A. Serum and glucocorticoid-responsive kinase-1 regulates cardiomyocyte survival and hypertrophic response. *Circulation* 2005;**111**:1652–1659.
35. Song M, Matkovich SJ, Zhang Y, Hammer DJ, Dorn GW II. Combined cardiomyocyte PKCdelta and PKCepsilon gene deletion uncovers their central role in restraining developmental and reactive heart growth. *Sci Signal* 2015;**8**:ra39.
36. Volkens M, Konstandin MH, Doroudgar S, Toko H, Quijada P, Din S, Joyo A, Ornelas L, Samse K, Thuerauf DJ, Gude N, Glembotski CC, Sussman MA. Mechanistic target of rapamycin complex 2 protects the heart from ischemic damage. *Circulation* 2013;**128**:2132–2144.
37. Shimobayashi M, Hall MN. Making new contacts: the mTOR network in metabolism and signalling crosstalk. *Nat Rev Mol Cell Biol* 2014;**15**:155–162.
38. Sarbassov DD, Ali SM, Kim DH, Guertin DA, Latek RR, Erdjument-Bromage H, Tempst P, Sabatini DM. Rictor, a novel binding partner of mTOR, defines a rapamycin-insensitive and raptor-independent pathway that regulates the cytoskeleton. *Curr Biol* 2004;**14**:1296–1302.
39. Facchinetti V, Ouyang W, Wei H, Soto N, Lazorchak A, Gould C, Lowry C, Newton AC, Mao Y, Miao RQ, Sessa WC, Qin J, Zhang P, Su B, Jacinto E. The mammalian target of rapamycin complex 2 controls folding and stability of Akt and protein kinase C. *EMBO J* 2008;**27**:1932–1943.
40. Li W, Zhang J, Bottaro DP, Pierce JH. Identification of serine 643 of protein kinase C-delta as an important autophosphorylation site for its enzymatic activity. *J Biol Chem* 1997;**272**:24550–24555.
41. Parekh D, Ziegler W, Yonezawa K, Hara K, Parker PJ. Mammalian TOR controls one of two kinase pathways acting upon nPKCdelta and nPKCepsilon. *J Biol Chem* 1999;**274**:34758–34764.
42. Basu A, Sridharan S, Persaud S. Regulation of protein kinase C delta downregulation by protein kinase C epsilon and mammalian target of rapamycin complex 2. *Cell Signal* 2009;**21**:1680–1685.
43. Gallegos LL, Newton AC. Spatiotemporal dynamics of lipid signaling: protein kinase C as a paradigm. *IUBMB Life* 2008;**60**:782–789.
44. Freeley M, Kelleher D, Long A. Regulation of protein kinase C function by phosphorylation on conserved and non-conserved sites. *Cell Signal* 2011;**23**:753–762.
45. Liu Q, Chen X, Macdonnell SM, Kranias EG, Lorenz JN, Leitges M, Houser SR, Molkentin JD. Protein kinase C(alpha), but not PKC(beta) or PKC(gamma), regulates contractility and heart failure susceptibility: implications for ruboxistaurin as a novel therapeutic approach. *Circ Res* 2009;**105**:194–200.
46. Cornu M, Albert V, Hall MN. mTOR in aging, metabolism, and cancer. *Curr Opin Genet Dev* 2013;**23**:53–62.
47. Mayr M, Chung YL, Mayr U, McGregor E, Troy H, Baier G, Leitges M, Dunn MJ, Griffiths JR, Xu Q. Loss of PKC-delta alters cardiac metabolism. *Am J Physiol Heart Circ Physiol* 2004;**287**:H937–H945.
48. Mayr M, Metzler B, Chung YL, McGregor E, Mayr U, Troy H, Hu Y, Leitges M, Pachinger O, Griffiths JR, Dunn MJ, Xu Q. Ischemic preconditioning exaggerates cardiac damage in PKC-delta null mice. *Am J Physiol Heart Circ Physiol* 2004;**287**:H946–H956.
49. Godel M, Hartleben B, Herbach N, Liu S, Zschiedrich S, Lu S, Debreczeni-Mor A, Lindenmeyer MT, Rastaldi MP, Hartleben G, Wiech T, Fornoni A, Nelson RG, Kretzler M, Wanke R, Pavenstadt H, Kerjaschki D, Cohen CD, Hall MN, Ruegg MA, Inoki K, Walz G, Huber TB. Role of mTOR in podocyte function and diabetic nephropathy in humans and mice. *J Clin Invest* 2011;**121**:2197–2209.
50. Hietakangas V, Cohen SM. Re-evaluating AKT regulation: role of TOR complex 2 in tissue growth. *Genes Dev* 2007;**21**:632–637.
51. Shiojima I, Yefremashvili M, Luo Z, Kureishi Y, Takahashi A, Tao J, Rosenzweig A, Kahn CR, Abel ED, Walsh K. Akt signaling mediates postnatal heart growth in response to insulin and nutritional status. *J Biol Chem* 2002;**277**:37670–37677.
52. Naga Prasad SV, Esposito G, Mao L, Koch WJ, Rockman HA. Gbetagamma-dependent phosphoinositide 3-kinase activation in hearts with in vivo pressure overload hypertrophy. *J Biol Chem* 2000;**275**:4693–4698.
53. Shioi T, McMullen JR, Kang PM, Douglas PS, Obata T, Franke TF, Cantley LC, Izumo S. Akt/protein kinase B promotes organ growth in transgenic mice. *Mol Cell Biol* 2002;**22**:2799–2809.
54. Condorelli G, Drusco A, Stassi G, Bellacosa A, Roncarati R, Iaccarino G, Russo MA, Gu Y, Dalton N, Chung C, Latronico MV, Napoli C, Sadoshima J, Croce CM, Ross J Jr. Akt induces enhanced myocardial contractility and cell size in vivo in transgenic mice. *Proc Natl Acad Sci USA* 2002;**99**:12333–12338.
55. Moschella PC, Rao VU, McDermott PJ, Kuppaswamy D. Regulation of mTOR and S6K1 activation by the nPKC isoforms, PKCepsilon and PKCdelta, in adult cardiac muscle cells. *J Mol Cell Cardiol* 2007;**43**:754–766.
56. Wang L, Rolfe M, Proud CG. Ca(2+)-independent protein kinase C activity is required for alpha1-adrenergic-receptor-mediated regulation of ribosomal protein S6 kinases in adult cardiomyocytes. *Biochem J* 2003;**373**:603–611.
57. McMullen JR, Shioi T, Zhang L, Tarnavski O, Sherwood MC, Dorfman AL, Longnus S, Pende M, Martin KA, Blenis J, Thomas G, Izumo S. Deletion of ribosomal S6 kinases does not attenuate pathological, physiological, or insulin-like growth factor 1 receptor-phosphoinositide 3-kinase-induced cardiac hypertrophy. *Mol Cell Biol* 2004;**24**:6231–6240.